Inorganic Chemistry Communications 48 (2014) 36–39

Contents lists available at ScienceDirect

Inorganic Chemistry Communications

journal homepage: www.elsevier.com/locate/inoche

A series of crystalline organic polymer–inorganic hybrid material zinc-phosphonate-phosphates synthesized in the presence of templates for superior performance catalyst support

Jing Huang [a,*], Jiali Cai [b], Chang Ming Li [c,*], Xiang Kai Fu [d]

[a] Research Center for Advanced Computation, School of Physics and Chemistry, Xihua University, Chengdu 610039, PR China
[b] College of Rongchang, Southwest University, Chongqing 402460, PR China
[c] Institute for Clean Energy & Advanced Materials, Southwest University, Chongqing 400715, PR China
[d] College of Chemistry and Chemical Engineering, Southwest University, Chongqing 400715, PR China

ARTICLE INFO

Article history:
Received 17 June 2014
Received in revised form 2 August 2014
Accepted 6 August 2014
Available online 7 August 2014

Keywords:
Zinc poly(styrene-phenylvinylphosphonate)-phosphate
Salen Mn(III)
Heterogeneous catalysts
Asymmetric epoxidation
Hybrid material

ABSTRACT

New types of organic copolymer–inorganic hybrid material zinc-phosphonate-phosphates are prepared with amines as templates. Notably, crystalline samples are obtained not with traditional methods but with simple reactions. Moreover, the samples are provided with the potential application as superior performance catalyst supports.

Introduction

Since the first synthesis of aluminium phosphate zeolites in 1982 [1], considerable interests have been focused on various metal phosphate materials [2]. Metal phosphonates exhibit a variety of open frameworks such as layered and microporous structures [3]. Materials with open framework and microporous structures are expected to find their use as hybrid composite materials in electro-optical and sensing applications in the future [4]. Research in the field of zirconium phosphates and zirconium phosphonates is very intense, which have involved mainly adsorbent [5–7], inorganic ion exchangers [8,9], intercalation chemistry [10,11], sensor and proton conductivity [12] and catalysis [13–15]. Our group has devoted ourselves to these in the last decades. Zirconium oligostyrenylphosphonate-phosphate (ZSPP) and zirconium poly(styrene-phenylvinylphosphonate)-phosphate (ZPS-PVPA) were prepared and used as catalyst supports. The immobilized catalysts display higher conversions, enantioselectivities and reusabilities than those achieved with the homogeneous catalysts under the same reaction conditions [16–22]. In addition, zinc phosphates have been proven to be very versatile in the formation of organic–inorganic hybrid materials [23,24]. In this work, a series of new types of organic copolymer–inorganic hybrid material zinc phosphonate-phosphate are prepared in the presence of templates (Scheme 1). The question as to whether or not crystalline zinc-phosphonate-phosphate hybrid materials could also be synthesized without the appending of templates and the roles of the templates as well as the feasibility for the superior catalyst performance supports are all examined here.

Results and discussion

The sodium content in sample 1e is 1.7%, which is 0.2% lower than that of theoretical values. This could be attributed to the surface-bound or intercalated water leading to the augment of the molecular weight.

According to FT-IR spectra (Fig. S1), the strong and wide absorption bands extending from 3100 to 3700 cm^{-1} and centering at 3500 cm^{-1} are assigned to the –OH, which verify the presence of H-bound interactions between the aminonium ion and pendant HPO_4^- group. The prominent bands at 1145, 1089, and 986 cm^{-1} are attributed to $R-PO_3^{2-}$ stretching vibrations. The absorptions at 1201, 1144, and 1077 cm^{-1} are due to the phosphonate and phosphate stretching vibrations.

On account of the TG curves (Fig. S2), samples 1a–1f lose 2.0–3.5 mol equivalents of surface-bound or intercalated water below 200 °C. There are two types of weight loss for these samples. According to samples 1a–1d, the surface-bound or intercalated water is firstly lost, followed by

* Corresponding authors.
E-mail address: hj41012@163.com (J. Huang).

http://dx.doi.org/10.1016/j.inoche.2014.08.006
1387-7003/

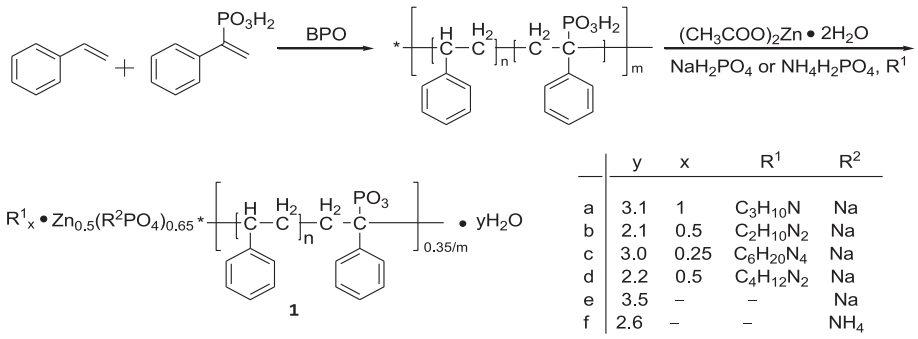

	y	x	R^1	R^2
a	3.1	1	$C_3H_{10}N$	Na
b	2.1	0.5	$C_2H_{10}N_2$	Na
c	3.0	0.25	$C_6H_{20}N_4$	Na
d	2.2	0.5	$C_4H_{12}N_2$	Na
e	3.5	–	–	Na
f	2.6	–	–	NH_4

Scheme 1. Synthesis of 1.

the decomposition of the templates, and then the sharp weight loss is in the temperature range of 200–600 °C, owing to the decomposition of the appended organic fragments. Finally, the small weight loss between 600 °C and 1000 °C is due to phase changes from layer to cubic $Zn_2P_2O_7$ and $NaZnPO_4$. While for samples 1e and 1f, the weight loss processes are similar to those of 1a–1d apart from the absence of the decomposition of the templates. On the other hand, organic reactions are usually carried out below 200 °C. Therefore, the samples are provided with enough thermal stabilities as catalyst supports.

XRD patterns (Fig. S3) indicate that 1a–1f are in crystalline states and could be served as mesoporous materials. Simultaneously, the interlayer distances of samples 1a–1f are approximately 11 Å, which are broader than those of inorganic zinc phosphate $Zn_3(PO_4)_2$ (10.61 Å). It may be that the styrene-phenylvinylphosphonic acid copolymer chains in the samples make the zinc layer stretched and becoming broader. Moreover, pores or channels of various sizes and shapes are formed by appropriate modification of the styrene-phenylvinylphosphonic acid copolymer chain, further giving birth to a significant impact on the excellent catalytic activity. The interlayer distance of sample 1f is a little narrower than that of the other samples, owing to the ammonium dihydrogen phosphate as the inorganic phosphate resource.

The diffuse reflectance UV–vis spectrums for samples 1a–1f (Fig. S4) show a strong absorption around 227 nm, which may be assigned to the π–π* transition of the phenyl groups. Another strong absorption is shown around 326 nm. The phenomenon may be originated in two aspects of reasons. For samples 1a–1d, this may be attributed to the involvement of the charge transfer transitions from the N atoms of the templates to the empty 4s orbitals of the Zn^{2+} ions, while for samples 1e and 1f, this perhaps is due to the O atoms of the phosphate or phosphonate to the empty 4s orbitals of the Zn^{2+} ions.

Based on the desorption isotherm (Fig. 1), sample 1c indicates a hierarchical distribution of pore size. The pore diameters of the particles are mainly between 15 Å and 30 Å, and some other particles vary from 3 nm to 30 nm as well as few particles are over 30 nm in diameter.

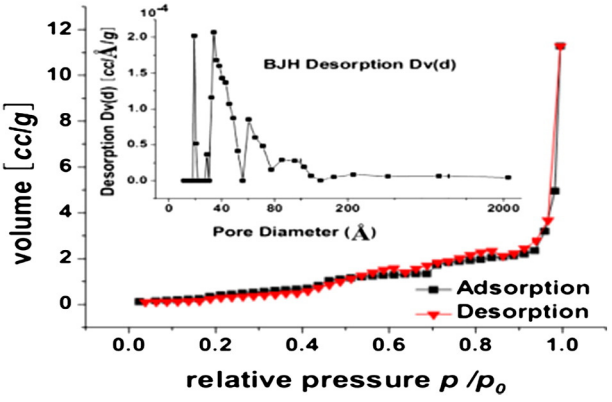

Fig. 1. The nitrogen adsorption–desorption isotherm and pore distribution of sample 1c.

Meanwhile, the size of solvated Mn(salen)Cl complex is estimated to be 2.05–1.61 nm by MM2 based on the minimized energy [25]. On the basis of this, sample 1c could provide enough room to accommodate the solvated chiral Mn(III) salen complex. In addition, the local environment inside the mesopores and pore size of the support definitely put effect on the enantioselectivity of the epoxidation. It is the crucial property that makes these samples being superior performance catalyst supports.

Compared with sample 1e, different templates played different impacts on samples 1a–d such as the physical properties of 1a–f in Table 1.

In Fig. 2, the different morphologies of the samples are attributed to the templates and inorganic phosphate resources. As seen in sample 1a, it is consisted irregularly of many platy layers, owing to the presence of the parts of zinc phosphonate in it. The anomalous clusters are induced by accumulation of the fraction of zinc phosphate in it. With regard to sample 1c, the mixed powders of atypical particles and hexagonal bipyramid particles as well as anomalous suborbicular particles could be discerned, and for sample 1e, there are regular neat plate layers which are mainly aggregation of the parts of zinc phosphate in it, while the anomalous roughly spherical segments are congregation of the proportion of zinc poly(styrene-phenylvinylphosphonate) in it. The appearances shed light not only on the intricate relationship among the open framework phosphates of different dimensionalities, but also on the mechanism of formation of the complex structures. Meanwhile, the supports possess various caves, holes, porous and channels. Some micropores and secondary channels would increase the surface area of the catalyst and provide enough chance for substrates to access to the catalytic active sites. While for sample 1f, it is abnormally made up of lamellar sections and clusters. In a word, both various templates and different inorganic phosphate resources play vital impacts on the appearances of the samples and further influence the structure of the catalysts as well as the catalytic abilities.

TEM photographies of sample 1a (Fig. 3) manifest that the configuration is filiform in structure and the sample consists of many irregular particles, while for sample 1e (Fig. 4), the structure of the support is spheroid and their sizes are about 70–80 nm. The channels, holes and cavums could be observed clearly. Meanwhile, the average diameter of these secondary channels among the layers of the supports is around 50–60 nm. Based on the interlayer distance of the sample determined

Table 1
The physical properties of 1a–f.

Sample	Surface area (m^2/g)	Pore volume ($\times 10^{-2}$ cm^3/g)	Average pore diameter (nm)
1a	3.8	1.5	2.1
1b	4.6	1.8	3.1
1c	5.1	2.0	3.6
1d	4.4	1.9	3.3
1e	4.8	1.2	3.4
1f	4.9	1.3	3.5

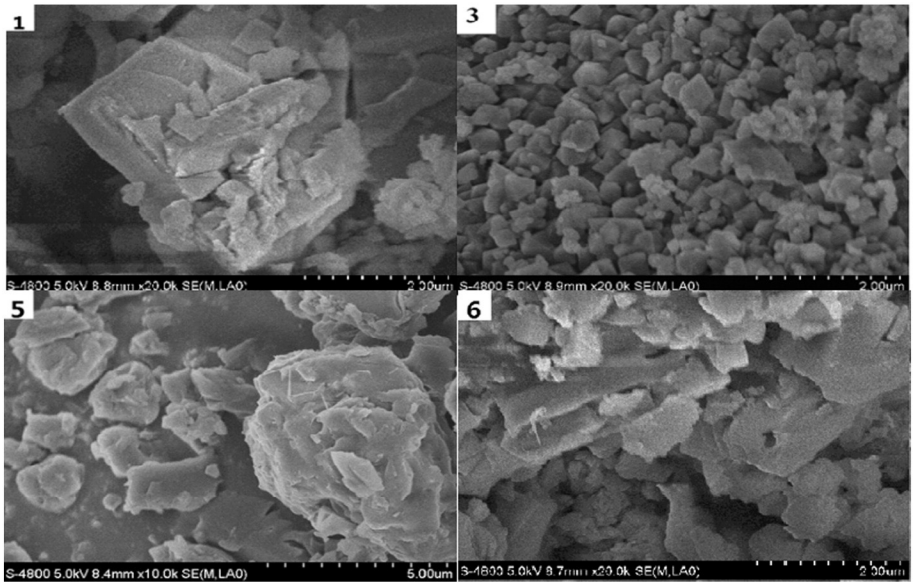

Fig. 2. SEM images of samples (1) 1a, (3) 1c, (5) 1e and (6) 1f.

by XPRD, it could be deduced that each particle is made up of stacks of 25–30 layers. Therefore, more chances would be provided for substrates to transfer to the internal catalytic active sites and further result in the superior catalytic ability.

The activities of the catalysts (Scheme 2) for asymmetric epoxidation of unfunctional olefins are presently in progress. The primary results are summarized in Table 2. Obviously, the activities of catalysts A, C and D are more superior than that of catalyst B, which is partly due to the templates. Further researches are under way.

Conclusions

In summary, a series of crystalline organic polymer–inorganic hybrid materials zinc-phosphonate-phosphates have been synthesized with amines as the templates. Owing to the templates and inorganic phosphate resource, the samples show versatile properties and could be used as superior performance catalyst supports. Furthermore, chiral salen Mn(III) deposited compounds are stable, effective and promising catalysts and may be provided with potential industry application.

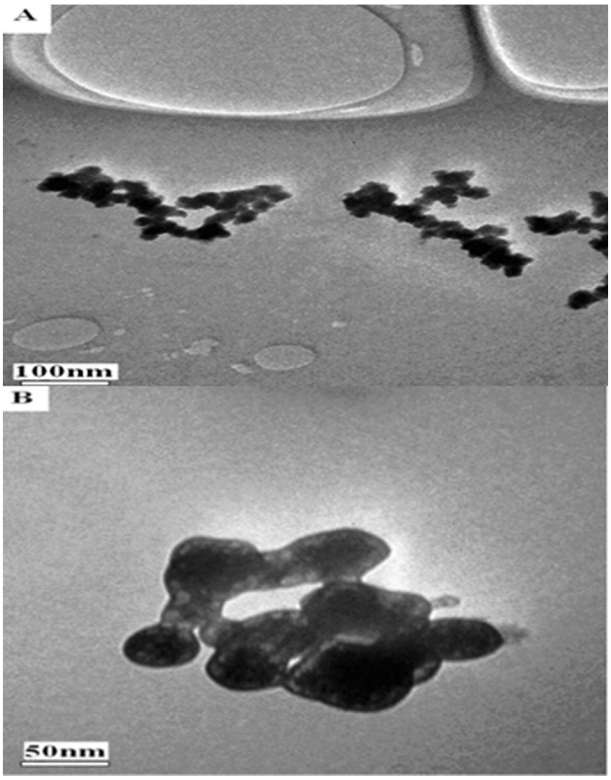

Fig. 3. TEM images of sample 1a (A and B).

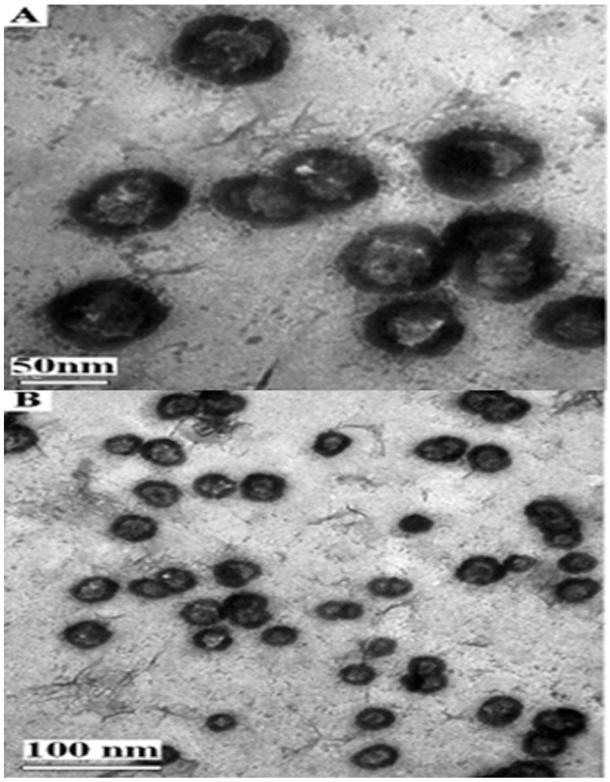

Fig. 4. TEM images of sample 1e (A and B).

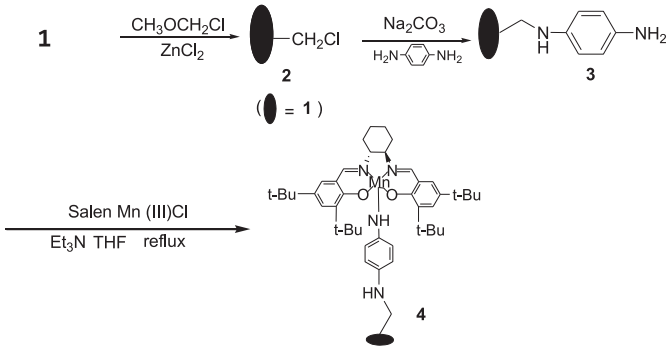

Scheme 2. Synthesis of the catalyst.

Table 2
Asymmetric epoxidation of α-methylstyrene and indene catalyzed by heterogeneous catalysts with m-CPBA/NMO[m] as oxidant systems.

Entry	Substrate	Catalyst	Time	Con. (%)	ee (%)
1	α-Methylstyrene	A	6	99.2	99.5
2	Indene	A	6	99.4	99.6
3	Indene	B	6	62	59
4	α-Methylstyrene	B	6	56	18
5	α-Methylstyrene	C	6	96.2	94.7
6	α-Methylstyrene	D	6	98.8	87.6

A = the immobilized chiral salen Mn(III) catalysts on *p*-phenylenediamine modified sample 1a.
B = the immobilized chiral salen Mn(III) catalysts on *p*-phenylenediamine modified ZPS-IPPA (zirconium poly (styrene-isopropylenephosphonate)-phosphate).
C = the immobilized chiral salen Mn(III) catalysts on *p*-phenylenediamine modified sample 1b.
D = the immobilized chiral salen Mn(III) catalysts on *p*-phenylenediamine modified sample 1f.
[m] Reactions were carried out at −20 °C in CH_2Cl_2 (4 ml) with α-methylstyrene (1 mmol) or indene (1 mmol), *n*-nonane (internal standard, 1 mmol), NMO (5 mmol), homogeneous (5 mol%) or heterogeneous salen Mn(III) catalysts (5 mol%) and *m*-CPBA (2 mmol). The conversion and the ee value were determined by GC with chiral capillary columns (HP19091G-B213, 30 m × 0.32 mm × 0.25 μm).

Acknowledgment

This work was financially supported by the Fundamental Research Funds for the Central Universities (XDJK2013C120), the Xihua University Key Projects (Z1223321), Sichuan Province Applied Basic Research Projects (2013JY0090) and the Department of Education of Sichuan Province Projects (13ZB0030).

Appendix A. Supplementary material

Supplementary data to this article can be found online at http://dx.doi.org/10.1016/j.inoche.2014.08.006.

References

[1] S.T. Wilson, B.M. Lok, C.A. Messina, T.R. Cannan, E.M. Flanigan, Aluminophosphate molecular sieves: a new class of microporous crystalline inorganic solids, J. Am. Chem. Soc. 104 (1982) 1146–1147.
[2] T.J. Russin, E.İ. Altınoğlu, J.H. Adair, P.C. Eklund, Measuring the fluorescent quantum efficiency of indocyanine green encapsulated in nanocomposite particulates, J. Phys. Condens. Matter 22 (2010) 334217.
[3] Y.C. Chen, K.B. Han, H. Mizukami, A. Wojcik, A. Ostafin, Fade and quench-resistant emission in calcium phosphate nanoreactors, Nanotechnology 21 (2010) 455701.
[4] Y.H. Kim, B.T. Lee, Novel approach to the fabrication of an artificial small bone using a combination of sponge replica and electrospinning methods, Sci. Technol. Adv. Mater. 12 (2011) 035002.
[5] A. Clearfield, D.S. Thakur, Zirconium and titanium phosphates as catalysts: a review, Appl. Catal. A Gen. 26 (1986) 1–26.
[6] S. Nakayama, K. Itoh, Effect of weight loss on liquid-phase-sintered silicon carbide, J. Eur. Ceram. Soc. 23 (2003) 1047–1052.
[7] T.M. Suzuki, S. Kobayashi, D.A. Pacheco Tanaka, M.A. Llosa Tanco, T. Nagase, Y. Onodera, Separation and concentration of trace Pb(II) by the porous resin loaded with α-zirconium phosphate crystals, React. Funct. Polym. 58 (2004) 131–138.
[8] A.A. Marti, J.L. Colon, Direct Ion exchange of tris(2,2′-bipyridine)ruthenium(II) into an α-zirconium phosphate framework, Inorg. Chem. 42 (2003) 2830–2832.
[9] K.M. Parida, B.B. Sahu, D.P. Das, A comparative study on textural characterization: cation-exchange and sorption properties of crystalline α-zirconium(IV), tin(IV), and titanium(IV) phosphates, J. Colloid Interface Sci. 270 (2004) 436–445.
[10] C.V. Kumar, A. Chaudhari, Proteins immobilized at the galleries of layered α-zirconium phosphate: structure and activity studies, J. Am. Chem. Soc. 122 (2000) 830–837.
[11] U. Costantino, M. Nocchetti, R. Vivani, Preparation, characterization, and structure of zirconium fluoride alkylamino-N, N-bis methylphosphonates: a new design for layered zirconium diphosphonates with a poorly hindered interlayer region, J. Am. Chem. Soc. 124 (2002) 8428–8434.
[12] G. Alberti, M. Casciola, Solid state protonic conductors, present main applications and future prospects, Solid State Ionics 145 (2001) 3–16.
[13] I.O. Benftez, B. Bujoli, L.J. Camus, C.M. Lee, F. Odobel, D.R. Talham, Monolayers as models for supported catalysts: zirconium phosphonate films containing manganese(III) porphyrins, J. Am. Chem. Soc. 124 (2002) 4363–4370.
[14] I.C. Marcu, I. Sandulescu, J.M.M. Millet, Oxidehydrogenation of *n*-butane over tetravalent metal phosphates based catalysts, Appl. Catal. A Gen. 227 (2002) 309–320.
[15] M. Curini, F. Montanari, O. Rosati, E. Lioy, R. Margarita, Layered zirconium phosphate and phosphonate as heterogeneous catalyst in the preparation of pyrroles, Tetrahedron Lett. 44 (2003) 3923–3925.
[16] A. Corma, H. García, F.X.L. Xamena, Engineering metal organic frameworks for heterogeneous catalysis, Chem. Rev. 110 (2010) 4606–4655.
[17] D.K. Garner, L. Liang, D.A. Barrios, J.L. Zhang, Y. Lu, The important role of covalent anchor positions in tuning catalytic properties of a rationally designed MnSalen-containing metalloenzyme, ACS Catal. 1 (2011) 1083–1089.
[18] L. Kollár, P-heterocycles as ligands in homogeneous catalytic reactions, Chem. Rev. 110 (2010) 4257–4302.
[19] C.S. Yeung, V.M. Dong, Catalytic dehydrogenative cross-coupling: forming carbon–carbon bonds by oxidizing two carbon–hydrogen bonds, Chem. Rev. 111 (2011) 1215–1292.
[20] J. Huang, X.K. Fu, G. Wang, Q. Miao, G.M. Wang, Axially coordinated chiral salen Mn(III) anchored onto azole onium modified ZnPS-PVPA as effective catalysts for asymmetric epoxidation of unfunctionalized olefins, Dalton Trans. 41 (2012) 10661–10669.
[21] B.W. Gong, X.K. Fu, J.X. Chen, Y.D. Li, X.C. Zou, X.B. Tu, P.P. Ding, L.P. Ma, Synthesis of a new type of immobilized chiral salen Mn(III) complex as effective catalysts for asymmetric epoxidation of unfunctionalized olefins, J. Catal. 262 (2009) 9–17.
[22] J.L. Cai, J. Huang, C.M. Li, H. Feng, Z.G. Liu, Salen Mn(III) immobilized onto ZnPS-PVPA modified by 1,2,3-triazole as efficient and reusable catalysts for asymmetric epoxidation of olefins, RSC Adv. 3 (2013) 18661–18670.
[23] X. Shi, G. Zhu, S. Qiu, K. Huang, J. Yu, R. Xu, $Zn_2[(S)\text{-}O_3PCH_2NHC_4H_7CO_2]_2$: a homochiral 3D zinc phosphonate with helical channels, Angew. Chem. Int. Ed. 43 (2004) 6482–6485.
[24] J. Huang, X.K. Fu, G. Wang, C. Li, X.Y. Hu, Novel layered crystalline zinc poly (styrene-phenylvinyl phosphonate)-phosphate synthesized by a simple route in a THF–water medium, Dalton Trans. 40 (2011) 3631–3639.
[25] H.D. Zhang, C. Li, Asymmetric epoxidation of 6-cyano-2,2-dimethylchromene on Mn (salen) catalyst immobilized in mesoporous materials, Tetrahedron 62 (2006) 6640–6649.